

Naringenin-Based Oximes and Hydrazones: Synthesis, Molecular Docking with Bovine Serum Albumin and Drug-Likeness, Admet Profiling Studies

Ferhat Melihcan Abay¹ , Hafize Özcan^{2*} , Ayşen Şuekinci Yılmaz² , Ömer Zaim² 

¹ Trakya University, Institute of Natural and Applied Sciences, Edirne, 22030, Türkiye

² Trakya University, Faculty of Science, Department of Chemistry, Edirne, 22030, Türkiye

* hafizeozcan@trakya.edu.tr

* Orcid No: 0000-0002-8031-6755

Received: September 19, 2024

Accepted: January 13, 2025

DOI: 10.18466/cbayarfbe.1552978

Abstract

Scientists are now increasingly interested in the flavonoid molecule naringenin due to the broad spectrum of biological roles it conducts. Oximes and hydrazones were created employing derivatives of the naringenin-active substances 7-piperidinethoxy and 7-morpholinethoxy to contribute to this research. The ability of the produced compounds to bind to BSA was determined by molecular docking and their potential as medications was assessed using various methods. Based on Lipinski's rule of five, none of the substances were hazardous or carcinogenic, and their blood-brain barrier crossing values were all within permissible limits.

Keywords: BSA, Flavonoid, Hydrazones, Lipinski, Oximes

1. Introduction

Naturally occurring in citrus fruits, naringenin (4',5,7-trihydroxyflavone) belongs to the flavanone class of flavonoid compounds. Many biological and pharmacological activity studies with flavonoids have been going on for many years and have had impressive results [1-3]. In light of this relatively small amount of studies, scientists have started to research and find effective results on this flavanone skeleton namely naringenin which is well-known for its use in biochemistry, food chemistry, medicine, and cosmetics [4-6]. Based on their activities, many naringenin derivatives have been produced and their biological effects have been studied in various areas. Studies on them showed that they have antiviral, anticancer, antioxidant, anti-inflammatory, antidiabetic, and anti-atherogenic activities [7-10].

The C-7- derivatives of naringenin are the most studied ones. Research with these derivatives has shown that C-7-alkyl derivatives exhibit significant biological activity against many microorganisms and anticancer cell lines [7, 11]. Morpholine or piperazine-linked 7-O-naringenin derivatives were chosen as this study's starting material. Literature investigations indicated that the biological activities of naringenin derivatives were further boosted

by the carbonyl group converted to oxime in addition to the alkyl groups [12, 13]. In this direction, we first aimed to synthesize the oximes and hydrazones of 7-O-naringenin derivatives (**3a** and **3b**) whose activity was shown previously (Figure 1).

The interaction of the molecules with the proteins in the blood plasma determines their pharmacological and pharmacokinetic characteristics. Serum albumins, one of the most essential proteins, account for 60 percent of all plasma proteins. These proteins carry out physiological tasks such as transporting endogenous and exogenous substances, maintaining osmotic blood pressure, and helping to keep blood pH [14]. The binding interaction of serum albumin with drugs controls pharmaceuticals' transportation, distribution, and metabolism in vivo. Stronger serum albumin-drug interactions are generally thought to result in a reduction in the concentration of free medication in plasma. In contrast, weaker interactions may result in a shorter half-life or inadequate pharmaceutical dispersion in vivo. Understanding how a drug interacts with and binds to serum albumin provides crucial insight into how it works in vivo [15]. Bovine serum albumin (BSA) has become among the most extensively researched proteins due to its accessibility, low cost, and 75.8% similarity to human serum albumin (HSA). BSA is heart-shaped and made up three main

domains (I, II, and III) and their sub-domains (A and B). Research on the relationship between flavonoids and serum albumin has become increasingly important in the pharmaceutical industry, and a variety of papers are available in the literature on this topic. [16].

Regarding this viewpoint, the purpose of the current study was to clarify the molecular docking-based interactions and binding of two oximes and two hydrazone derivatives of the 7-O-alkyl naringenin with BSA. Additionally, in-silico investigations of the synthesized compounds' ADMET (Absorption, Distribution, Metabolism, Excretion, Toxicity) were carried out, and Lipinski's rule of five filters was used to calculate their drug potentials.

2. Materials and Methods

2.1. General

All reagents were purchased from Sigma-Aldrich or Merck. Merck silica gel (60 mesh) was used for column chromatography and Merck silica gel plates (60F-254) for TLC analysis. Reactions were mainly carried out in an inert atmosphere. The progress of the reactions was monitored using TLC with methanol and chloroform as eluents. The IR spectra were recorded using an FT-IR spectrophotometer, and the ^1H NMR spectra were acquired in DMSO- d_6 using a Varian Mercury Plus 400 MHz spectrometer. ^{13}C NMR spectra were acquired at room temperature using a 100 MHz spectrometer. In ^1H NMR, the following acronyms are used: s = singlet, br. s = broad singlet, d = doublet, dd = doublet of doublets, t = triplet, qui = quintet, and m = multiplet. High-resolution mass spectra (HR-MS) were obtained in AB SCIEX 4600 Q-TOF (Ab Sciex, USA) in m/z (rel.%).

2.2. Synthesis of 7-(2-Bromoethoxy)-5-hydroxy-2-(4-hydroxyphenyl) chroman-4-one (2)

7-(2-bromoethoxy)-5-hydroxy-2-(4-hydroxyphenyl) chroman-4-one was synthesized via a procedure that we utilized previously [7].

2.3. General Procedure for Preparation of Naringenin Alkylamines (3a-3b)

In a solution of compound **2** (300 mg, 0.79 mmol, 1 eq.) in dry acetonitrile (45 mL), piperidine or morpholine (0.87 mmol, 1.1 eq.) and potassium carbonate (0.87 mmol, 1.1 eq.) were added, and the temperature was brought to 70°C. The progress of the reaction was monitored by TLC. After the reaction was terminated, acetonitrile was evaporated and the crude product was purified with flash column chromatography on silica gel using dichloromethane: methanol (19:1). The spectroscopic data were in agreement with literature values [7].

2.4. General Procedure for Preparation of Naringenin Oximes and Hydrazones

0.525 mmol of compound **3a** or **3b** and 1.25 mmol of sodium acetate were mixed with 5 mL of methanol using a magnetic stirrer in a nitrogen atmosphere. Hydroxylamine or hydrazine (1.28 mmol) was added to the solution and stirred at 40 °C for 24 hours. It was then refluxed for a day. The resulting mixture was poured into ice water, and the solids were filtered and dried.

2.4.1. (E)-7-(2-piperidinoethoxy)-5-hydroxy-2-(4-hydroxyphenyl) chroman-4-hydrazone (4a)

Yield 50%, ^1H NMR (400 MHz, DMSO- d_6 , δ , ppm): 12.91 (s, 1H), 9.54 (s, 1H), 7.27 (d, $J = 8.5$ Hz, 2H), 6.76 (d, $J = 8.5$ Hz, 2H), 6.35 (s, 2H), 5.95 (m, 2H), 5.04 (dd, $J = 11.9$, 3.1 Hz, 1H), 4.04 (t, $J = 5.9$ Hz, 2H), 3.1 (dd, $J = 11.9$ Hz, 3.1 Hz, 1H), 2.58 (m, 3H), 2.38 (t, $J = 5.5$ Hz, 4H), 1.46 (m, 4H), 1.35 (qui, $J = 5.9$ Hz, 2H). ^{13}C NMR (100 MHz, DMSO- d_6 , δ , ppm): 160.2, 159.9, 157.9, 157.4, 145.7, 130.6, 128.4, 115.51, 100.6, 96.1, 93.9, 76.4, 65.9, 57.6, 54.6, 30.7, 25.8, 24.2. IR (cm^{-1}): 2938, (C-H), 1616(C=N), 1598, 1446 (C=C), 1199 (C-O), 1160 (C-N). HRMS: m/z $\text{C}_{22}\text{H}_{28}\text{N}_3\text{O}_4$ (M+H) $^+$ found: 398.2071; calc. 398.2080.

2.4.2. (E)-7-(2-morpholinoethoxy)-5-hydroxy-2-(4-hydroxyphenyl) chroman-4-hydrazone (4b)

Yield 57%, ^1H NMR (400 MHz, DMSO- d_6 , δ , ppm): 12.91 (s, 1H), 9.51 (s, 1H), 7.28 (d, $J = 8.1$ Hz, 2H), 6.77 (d, 2H), 6.35 (s, 2H), 6.00 – 5.93 (m, 2H), 5.02 (dd, $J = 11.8$, 3.1 Hz, 1H), 4.03 (t, $J = 5.9$ Hz, 2H), 3.55 (d, $J = 4.7$ Hz, 5H), 3.1 (dd, $J = 11.9$, 3.1 Hz, 1H), 2.6 (m, 3H), 2.42 (t, $J = 4.6$ Hz, 4H). ^{13}C NMR (100 MHz, DMSO- d_6 , δ , ppm): 160.12, 159.9, 157.8, 157.4, 145.8, 130.6, 128.4, 115.5, 100.6, 96.1, 94.2, 76.4, 66.7, 65.9, 57.3, 53.8, 30.4. IR (cm^{-1}): 2973, 2868 (C-H), 1614 (C=N), 1595, 1457 (C=C), 1202 (C-O), 1159 (C-N). HRMS: m/z $\text{C}_{21}\text{H}_{26}\text{N}_3\text{O}_5$ (M+H) $^+$ found: 400.1864; calc. 400.1872.

2.4.3. (E)-7-(2-piperidinoethoxy)-5-hydroxy-2-(4-hydroxyphenyl) chroman-4-oxime (5a)

Yield 27%, ^1H NMR (400 MHz, DMSO- d_6 , δ , ppm): 11.35 (s, 1H), 11.32 (s, 1H), 9.55 (d, $J = 8.4$ Hz, 1H) 7.27 (d, $J = 8.4$ Hz, 2H), 6.77 (dd, $J = 8.4$, 2.1 Hz, 2H), 6.08 (d, $J = 12.4$ Hz, 2H), 5.02 (d, $J = 11.5$ Hz, 1H), 4.25 (m, 2 H), 3.27 (m, 5H), 2.81(dd, $J = 7.2$, 11.8 Hz, 2H), 2.48 (m,2H), 1.76-1.61 (m, 3H), 1.48 (m, 2H). ^{13}C NMR (100 MHz, DMSO- d_6 , δ , ppm): 160.6, 159.4, 158.3, 157.8, 146.5, 130.1, 128.4, 115.48, 106.19, 95.79, 94.15, 76.5, 61.24, 54.36, 52.9, 29.7, 28.7, 22.6. IR (cm^{-1}): 3229 (O-H) 2988, 2902 (C-H), 1616 (C=N), 1577, 1457, 1373 (C=C), 1199 (C-O), 1156 (C-N). HRMS: m/z $\text{C}_{22}\text{H}_{27}\text{N}_2\text{O}_5$ (M+H) $^+$ found:399.1916; calc. 399.1919.

2.4.4. (*E*)-7-(2-morpholinoethoxy)-5-hydroxy-2-(4-hydroxyphenyl) chroman-4-oxime (**5b**)

Yield 90%, ¹H NMR (400 MHz, DMSO-d₆, δ, ppm): 11.31 (s, 1H), 11.24 (s, 1H), 9.5 (s, 1H), 7.2 (d, *J* = 8.4 Hz, 2H), 6.7 (d, *J* = 8.4 Hz, 2H), 5.99 (d, *J* = 4.6 Hz, 2H), 4.99 (dd, *J* = 11.7, 3.1 Hz, 1H), 4.02 (s, 2H), 3.54 (m, 5H), 3.3 (dd, *J* = 17.1, 3.2 Hz, 1H), 2.73 (dd, *J* = 17.1, 11.7 Hz, 2H), 2.49 (s, 4H). ¹³C NMR (100 MHz, DMSO-d₆, δ, ppm): 161.2, 159.4, 158.3, 157.95, 153.4, 130.1, 128.5, 115.6, 98.8, 96.1, 94.8, 76.4, 66.2, 56.9, 53.6, 43.2, 29.4. IR (cm⁻¹): 3240 (O-H), 2971, (C-H), 1614 (C=N), 1568, 1455, (C=C), 1196 (C-O), 1160 (C-N). HRMS: *m/z* C₂₁H₂₅N₂O₆ (M+H)⁺ found:401.1707; calc. 401.1712.

2.5. Molecular Docking

Molecular docking can be employed to replicate the ligand-protein interaction at the atomic level thereby it possible for us to better understand fundamental biological processes and identify how a ligand functions at the binding site of target proteins. Utilizing Auto Dock Tools 1. 5. 6 [17], molecular docking simulations of synthesized compounds were performed. BSA's crystal structure was obtained from Protein Databank (PDB ID:3V03). To prepare the protein for docking analysis, water molecules were deleted, and polar hydrogens and Kollman charges were added. The ligands were prepared for docking via the Chem3D program's molecular mechanics (MM2), which minimized their energy. The grid box was initially set to 126x126x126 for x, y, and z, respectively, and the best binding site was identified. The interactions were then thoroughly explored by readjusting the grid box to 60x60x60 for x, y, and z, respectively. Docking studies were carried out using the Lamarckian Genetic Algorithm (LGA). Eventually, among the nine docking interactions, the lowest energy ligand-protein binding was selected and analyzed. Ligand-protein interactions were simulated in Pymol [18] and Biovia Studio [19] programs.

2.6. Drug-Likeness Prediction

SwissADME was used to determine the drug-likeness study by computing the pharmacokinetic parameters of the compounds, eliminating and screening those that are incompatible. The Lipinski filter (Pfizer), which classifies small molecules based on physicochemical factors which includes Mw, H-bond acceptors, H-bond donors, TPSA, and log P is employed for this purpose [20]. The SwissADME program's Lipinski filter (Pfizer) was employed to examine the synthetic compounds' pharmacological similarities.

2.7. ADMET

ADMET server analyzes parameters such as Human

intestinal absorption (HIA), Metabolism, (CYP450) Inhibitors, carcinogenesis, Biodegradation of the test compound. (<http://lmm.d.ecust.edu.cn/admetserver/>). Using several models, the server predicts more than 50 ADMET parameters [21].

3. Results and Discussion

3.1. Chemistry

Naringenin contains three hydroxyl groups. The 4- and 7-hydroxy groups are easily available for O-substitutions, whereas the 5-hydroxy group is less accessible. When we compare the hydroxy groups, the 7-hydroxy group has more acidic hydrogen than the 4'-hydroxy group due to the hydroxy group's conjugation with the ketone. Starting with this knowledge, 1,2-dibromoethane was added to the mixture of (±)-naringenin (**1**) in acetone, resulting in a fair yield of 7-(2-Bromoethoxy)-5-hydroxy-2-(4-hydroxyphenyl)-chroman-4-one (**2**) with existing procedures [7] and then using the compound **2** and the proper amines (morpholine or piperazine) in acetonitrile, we started preparing two derivatives of 7-O-naringenin-amine. Next, to boost the molecule's ability to form more hydrogen bonds and to distinguish between its contacts, hydrazone and oxime derivatives of the related substance were created from each product. Oxime and hydrazone derivatives were obtained by adding sodium acetate along with hydroxylamine or hydrazine to morpholine and piperidine-containing derivatives of racemic naringenin, respectively. The spectral data of the synthesized molecules were evaluated by comparing them with naringenin oximes and hydrazones reported in the literature [13,22,23]. It was reported that when the ketone compound was converted to the oxime derivative, the carbonyl carbon and α carbon signals shifted to the upper field, and for α carbon, the ¹H and ¹³C δ-values of the *E*-configuration were lower than the *Z*-configuration. Based on these findings and the comparison of our NMR values with the *E* and *Z* naringenin oximes available in the literature, we believe that the configuration of the molecules we synthesized is *E* [22]. In addition, the NMR data of the obtained hydrazones were similar to the *E*-naringenin hydrazones in the literature [23].

For **4a**, (Figure 1) in the ¹H-NMR spectrum (Figure S1), the singlet 2H peak at 6.35 ppm represents the hydrogens in the N-NH₂ structure. The structure description of the rest of the molecule was detailed in our previous work [9]. The absence of a peak at 200-190 ppm in the ¹³C-NMR spectrum (Figure S2) proves the conversion of the carbonyl group to the imine structure, and the imine bond with the peak at 145.7 ppm is proven. The absence of a peak between 1800-1650 cm⁻¹ in the IR spectrum proves that the carbonyl group in **4a** has disappeared, while the

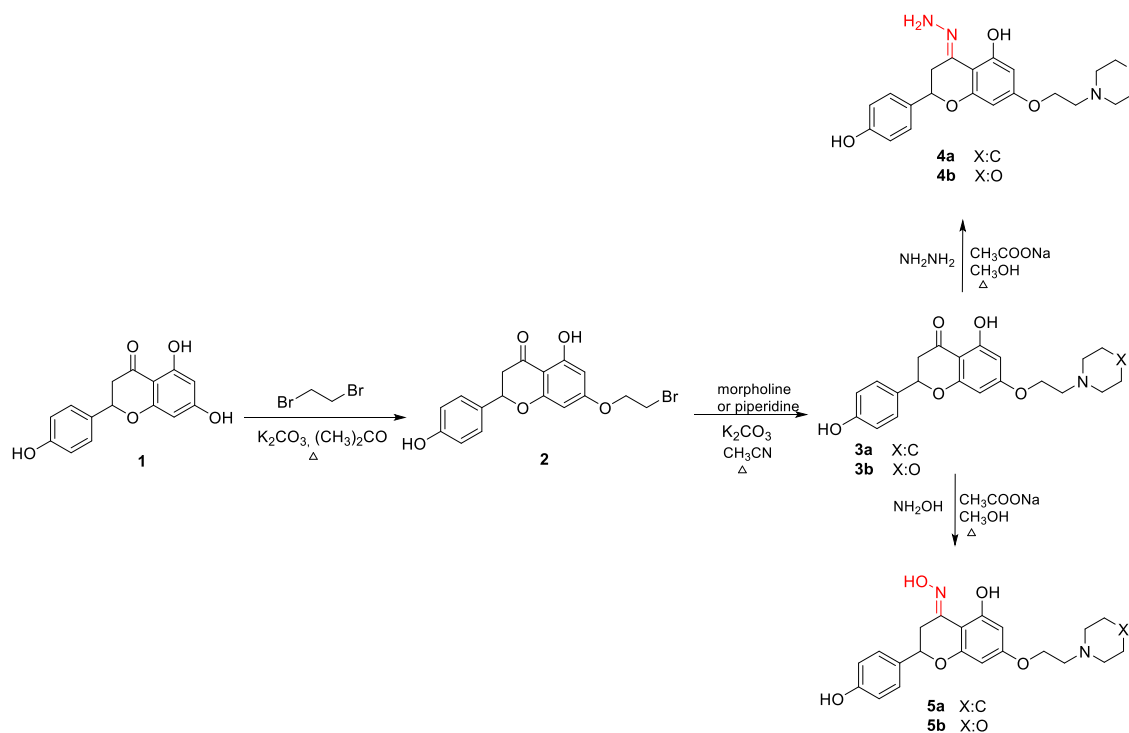


Figure 1. Synthesis of target oximes and hydrazones **4a-b** and **5a-b**

peak seen in the IR spectrum of 1616 cm^{-1} proves that the imine bond is formed. The MS value of the substance whose mass analysis was performed was found to be 398.2071 [M+H] and the value found is in agreement with the calculated value.

Similarly, for **5b**, it expresses the oxime -OH of the singlet peak at 11.31 ppm, and C5-OH of the singlet at 11.24 ppm in the $^1\text{H-NMR}$ spectrum. The singlet C5-OH peak, which was recorded at 12.08 ppm (for **3b**), moved to 11.24 ppm (for **5b**) after the C=O group was converted to the C=N group. This is because of the difference in the atom with which the H in C5-OH forms the H-bond. (Figure S13). In the $^{13}\text{C-NMR}$ spectrum (Figure S14), the peak showing the carbonyl group at 200-190 ppm disappeared, while the peak observed at 157.95 ppm corresponds to the oxime carbon. The absence of a peak between $1800\text{-}1650\text{ cm}^{-1}$ in the IR spectrum indicates the loss of the carbonyl group in the structure. The peak seen at 1614 cm^{-1} in the IR spectrum proves the formation of an oxime bond. 399.1916 observed in the mass spectrum was seen as [M+H] and the structure was confirmed.

Similar data were obtained for compounds **4b** and **5a**, consistent with the expected oxime and hydrazine structures.

3.2. Molecular Docking Analysis

The use of molecular docking simulations is a very efficient method for determining the structural compatibility of the investigated compounds and the

target macromolecules, their mode of interaction, binding energy, and chemical environment [24]. When the binding potential of flavonoids with BSA is examined, it was shown that different substituents greatly affect the binding ability of the molecules to BSA. Studies employing naringenin, which lacks functional groups, indicated that the binding energy to BSA was higher, whereas the binding energy of derivatives that could create more hydrogen bonds decreased. The molecules subject to our research can make more H-bonds and the molecular docking results of them with BSA, provide insights into the structural activity of them docked to a target biomolecule.

In the study of Hu et al. [25] the specific interaction of naringenin and BSA was investigated by spectroscopic methods including fluorescence spectroscopy and UV-visible absorption spectroscopy, and it was found that naringenin binds to BSA via hydrophobic interactions. Liu et al. [26] reported that naringenin's binding energy to BSA protein was 7.6 kcal/mol, it did not form hydrogen bonds, and it bound to the BSA through hydrophobic interactions. When the docking data were compared, it was seen that the oxime and hydrazone components of the designed naringenin derivatives reduced the binding energy by forming multiple hydrogen bonds.

The configurations of the naringenin derivatives-BSA complexes with the lowest binding energy are shown in Figure 2. Docking results revealed that all compounds bound inside the binding pocket in subdomain IB of BSA

Table 1. Binding energy and interactions of the compounds with BSA protein.

Docked Comp.	Binding Energy (kcal/mol)	Interacted residues	
		H-bond	Non-bonded
4a	-8.9	Asp108 O with H-N Asp108 O with H-N Leu112 N-H with O Leu112 O with H-O	Pro110, Arg144 π -Alkyl His145, Ala193 Alkyl Ser109 Amide- π Glu424 π -Anion Arg458 π -Cation
4b	-8.6	Leu112, N-H with O His145 N-H with O His145 N-H with N Ser192 O with H-N Ser192 H with O	Pro110, Arg144 π -Alkyl His145, Ala193 Alkyl Ala193 π -Sigma Arg458 π -Cation
5a	-8.8	Asp108 O with H-O Arg458 O with H-O Leu112 N-H with O Leu112 O with H-O	Pro110, Arg144 π -Alkyl His145, Ala193, Leu454, Ile455 Alkyl Ser109 Amide- π Glu424 π -Anion Arg458 π -Cation
5b	-8.5	Asp 108 O with H-O Leu112 O with H-O	Pro110, Arg144 π -Alkyl His145, Ala193 Alkyl Ser109 Amide- π Glu424 π -Anion Asp458 π -Cation Arg458 N-H with H-O Arg458 N-H with H-O unfavorable donor-donor

with close binding energy (in the range of -8.5 / -8.9 kcal/mol). Amino acids in BSA bond with molecules via hydrogen bonds and hydrophobic interactions, as shown in Table 1. **4a** interacts with Asp108 and Leu112 via four hydrogen bonds, and **4b** interacts with Leu112, His145, and Ser192 amino acids via five hydrogen bonds. **5a** interacts with Asp108, Leu112, and Arg458 amino acids via four hydrogen bonds; **5b** interacts with Asp108 and Leu112 amino acids via two hydrogen bonds. We found that compounds **4a**, **5a**, and **5b** primarily functioned as hydrogen bond acceptors, whereas compound **4b** primarily functioned as a hydrogen bond donor. All molecules are surrounded by the Pro110 and Arg144 amino acids through π -alkyl interactions, His145 and Ala193 amino acids through alkyl interactions, and Ser109 amino acid through amide- π interactions. Additionally, although **4a**, **5a**, and **5b** interact with Glu424 amino acid via π -anion all compounds interact with Arg458 amino acid via π -cation. Finally, **5b** interacts with Arg458 amino acid through two unfavorable donor-donor interactions, so its binding energy is higher than other molecules. Multiple connections between derivatives and the BSA structure imply strong interactions and suggest that these substances can be delivered as medicinal products.

3.3. Drug-likeness Profiles

The druggability of the compounds and the corresponding radar plots are listed in Table 2. The six parameters studied by SwissADME [27], including lipophilicity, size, polarity, insolubility, saturation, and elasticity, are within the desired range as seen on the radar chart for all compounds.

In addition, all compounds obey Lipinski's rule of five [16]: number of H bond donors ≤ 5 , H bond acceptor ≤ 10 , molecular weight ≤ 500 , TPSA $\leq 140 \text{ \AA}^2$, $\log P \leq 5$. Compounds have enough hydrogen bond acceptors and donors to form hydrogen bonds. The mass of the compounds is within the desired range, and the presence of five rotatable bonds (should be less than ten) suggests molecular flexibility. They show strong permeability to the blood-brain barrier (BBB) and cellular plasma membrane, as topological polar surface area (TPSA) values are less than 140 \AA^2 . Octanol-water distribution coefficient (Log P), a metric for the hydrophilicity or hydrophobicity of molecules, shows that molecules with $\log P < 0$ have poor lipid bilayer permeability and those with $\log P > 3$ have poor water solubility. Log P values for them, which vary from 1.79 to 2.89, show that they are soluble in both water and lipids.

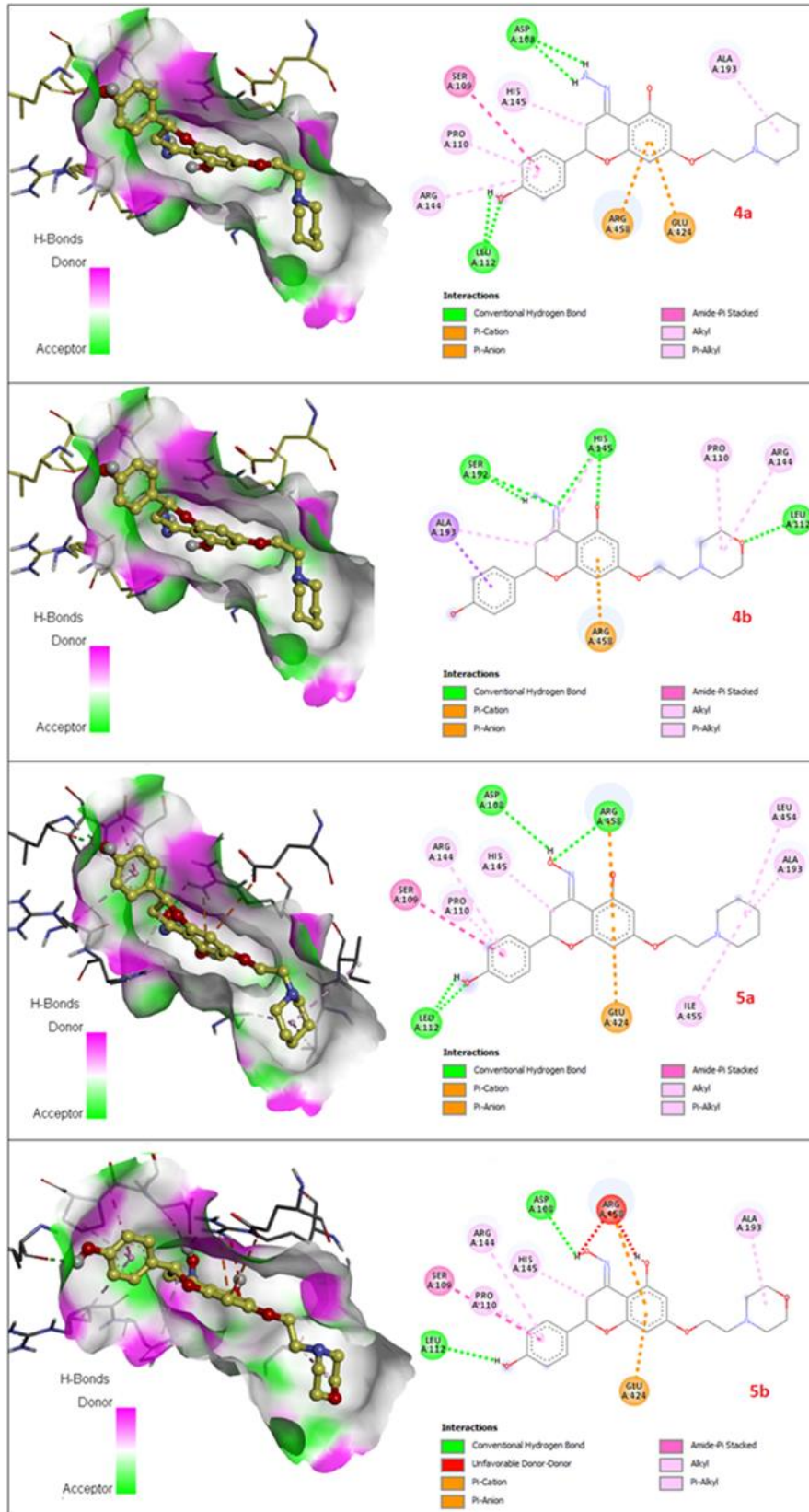
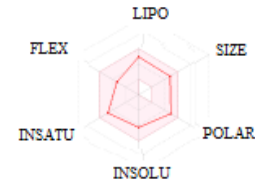
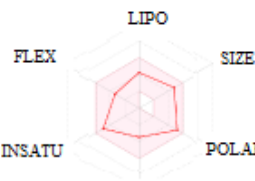
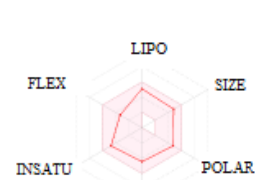


Figure 2. The lowest energy docked poses and 2D representations of the interactions of the **4a**, **4b**, **5a**, **5b** with bovine serum albumin.

Table 2. Druggability of Compounds.

Comp.	HBD ^[a]	HBA ^[b]	nROTB ^[c]	Lipinski, violation	TPSA ^[d] (Å ²)	MW ^[e]	logP ^[f]	Radar Chart
4a	3	6	5	Yes, 0	100.54	397.47	2.66	
4b	3	7	5	Yes, 0	109.77	399.44	1.79	
5a	3	7	5	Yes, 0	94.75	398,45	2.89	
5b	3	8	5	Yes, 0	103.98	400.43	2.03	

^[a] the number of H-bond donors, ^[b] the number of H-bond acceptors, ^[c] nROTB: the number of rotatable bonds, ^[d] Topological polar surface area, ^[e] Molecular Weight, ^[f] the octanol-water partition coefficient. In radar charts, the pink color shows the ideal range.

Table 3. ADMET profiling of the compounds.

	Absorption	Distribution	Metabolism (CYP450) Inhibitor					Excretion		Toxicity		
	HIA ^[a]	BBB ^[b]	2C19	3A4	2C9	2D6	1A2	B.D. ^[c]	C. ^[d]	Hp.T ^[e]	S.S ^[f]	AOT ^[g]
4a	82.30 (+)	0.675 (+)	No	No	No	No	No	NB ^[h]	No	No	No	III
4b	82.30 (+)	0.675 (+)	No	No	No	No	No	NB	No	No	No	III
5a	79.17 (+)	0.65 (+)	No	No	No	No	No	NB	No	No	No	III
5b	79.17 (+)	0.65 (+)	No	No	No	Yes	No	NB	No	No	No	III

^[a] Human Intestinal Absorption, ^[b] Blood Brain Barrier, ^[c] Biodegradation, ^[d] Carcinogenicity, ^[e] Hepatotoxicity, ^[f] Skin Sensitization, ^[g] Acute Oral Toxicity, ^[h] Non-biodegradable

3.4. ADMET Properties

The *in silico* predictions of the ADMET properties of the compounds are shown in Table 3. They can be absorbed by the human intestine and can cross the blood-brain barrier. This indicates the compounds have good potential for dispersion and absorption. The metabolic activity of the compounds was evaluated using a microsomal enzyme (Cytochrome P450 inhibitors), which catalyzes crucial drug metabolism processes. It can be seen from Table 3 that the compounds do not inhibit cytochrome P450, such as CYP: 1A2, 2C19, 2C9, 2D6, and 3A4, which cause drug interactions. The compounds are non-biodegradable nevertheless, they present no carcinogenicity, hepatotoxicity, or skin sensitization. They have type III (slightly toxic) acute oral toxicity (LD50) values, which are easily converted to type IV (nontoxic) during hit-lead optimization. According to the results, they have a good ADMET profile and are ideal candidates for medications.

4. Conclusion

In the study, two oximes and two hydrazones as derivatives of naringenin were synthesized, their geometries were clarified, and the binding interaction of each structure with BSA was investigated by molecular docking. The binding energies of the compounds were found to be in the range of -8.5 - 8.9 kcal/mol and the values were more effective than the molecular docking interactions of naringenin with BSA. In addition, the drug potentials of the molecules were investigated with SwissADME and admetSAR. The molecules complied with Lipinski's five rules, are not carcinogenic, hepatotoxic, skin-sensitizing properties, and the BBB values were within the range.

Acknowledgement

We gratefully acknowledge the financial support of the scientific research project commission of Trakya University (TÜBAP 2018/232).

Author's Contributions

Ferhat Melihcan Abay: Oxime and Hydrazone Preparation.

Hafize Ozcan: Data Analysis, Original draft preparation, Writing.

Ayşen Şuekinçi Yılmaz: Molecular Docking, ADMET predictions, Writing.

Ömer Zaim: Supervision, Reviewing and Editing.

Ethics

There are no ethical issues after the publication of this manuscript.

References

- [1]. Formica, J, Regelson, W. 1995. Review of the biology of quercetin and related bioflavonoids. *Food and Chemical Toxicology*; 33(12):1061-1080. [https://doi.org/10.1016/0278-6915\(95\)00077-1](https://doi.org/10.1016/0278-6915(95)00077-1).
- [2]. Cazarolli, LH, Zanatta, L, Alberton, EH, Bonorino, Figueiredo, MSR, Folador, P, Damazio, RG, et al. 2008. Flavonoids: prospective drug candidates. *Mini Reviews in Medicinal Chemistry*; 8(13):1429-1440. <https://doi.org/10.2174/138955708786369564>.
- [3]. Cushnie, TT, Lamb, AJ. 2011. Recent advances in understanding the antibacterial properties of flavonoids. *International Journal of Antimicrobial Agents*; 38(2):99-107. <https://doi.org/10.1016/j.ijantimicag.2011.02.014>.
- [4]. Miller, E, Schreier, P. Studies on flavonol degradation by peroxidase (donor: H₂O₂-oxidoreductase, EC 1.11. 1.7): Part 1—Kaempferol. *Food Chemistry*; 17(2):143-154. [https://doi.org/10.1016/0308-8146\(85\)90083-4](https://doi.org/10.1016/0308-8146(85)90083-4).
- [5]. Wiseman, H. 1996. Dietary influences on membrane function: importance in protection against oxidative damage and disease. *The Journal of Nutritional Biochemistry*; 7(1):2-15. [https://doi.org/10.1016/0955-2863\(95\)00152-2](https://doi.org/10.1016/0955-2863(95)00152-2).
- [6]. Hollman, P, Hertog, M, Katan, M. 1996. Role of dietary flavonoids in protection against cancer and coronary heart disease. *Biochemical Society Transactions*; 24:785-789. <https://doi.org/10.1042/bst0240785>.
- [7]. Zaim, Ö, Doğanlar, O, Zreigh, MM, Doğanlar, ZB, Özcan, H. 2018. Synthesis, Cancer-Selective Antiproliferative and Apoptotic Effects of Some (±)-Naringenin Cycloaminoethyl Derivatives. *Chemistry & Biodiversity*; 15(7):e1800016. <https://doi.org/10.1002/cbdv.201800016>.
- [8]. Hodek, P, Trefil, P, Stiborová, M. 2002. Flavonoids-potent and versatile biologically active compounds interacting with cytochromes P450. *Chemico-Biological Interactions*, 139(1):1-21. [https://doi.org/10.1016/S0009-2797\(01\)00285-X](https://doi.org/10.1016/S0009-2797(01)00285-X).
- [9]. Ahmadi, A, Hassandarvish, P, Lani, R, Yadollahi, P, Jokar, A, Bakar, SA, et al. 2016. Inhibition of chikungunya virus replication by hesperetin and naringenin. *RSC Advances*; 6(73):69421-69430. <https://doi.org/10.1039/C6RA16640G>.
- [10]. Denaro, M, Smeriglio, A, Trombetta, D. 2021. Antioxidant and anti-inflammatory activity of citrus flavanones mix and its stability after in vitro simulated digestion. *Antioxidants*; 10(2):140. <https://doi.org/10.3390/antiox10020140>.
- [11]. Babu, KS, Babu, TH, Srinivas, P, Kishore, KH, Murthy, U, Rao, JM. 2006. Synthesis and biological evaluation of novel C (7) modified chrysin analogues as antibacterial agents. *Bioorganic & Medicinal Chemistry Letters*; 16(1):221-2244. <https://doi.org/10.1016/j.bmcl.2005.09.009>.
- [12]. Zaim, Ö, Doğanlar, O, Doğanlar, ZB, Özcan, H, Zreigh, MM, Kurtdere, K. 2022. Novel synthesis naringenin-benzyl piperazine derivatives prevent glioblastoma invasion by inhibiting the hypoxia-induced IL6/JAK2/STAT3 axis and activating caspase-dependent apoptosis. *Bioorganic Chemistry*; 129:106209. <https://doi.org/10.1016/j.bioorg.2022.106209>.
- [13]. Türkan, B, Özyürek, M, Bener, M, Güçlü, K, Apak, R. 2012. Synthesis, characterization and antioxidant capacity of naringenin-oxime. *Spectrochimica Acta Part A: Molecular and Biomolecular Spectroscopy*; 85(1):235-240. <https://doi.org/10.1016/j.saa.2011.09.066>.

- [14]. Carter, DC, Ho, JX. 1994. Structure of serum albumin. *Advances in Protein Chemistry*; 45:153-203.
[https://doi.org/10.1016/S0065-3233\(08\)60640-3](https://doi.org/10.1016/S0065-3233(08)60640-3).
- [15]. Otagiri, M. 2005. A molecular functional study on the interactions of drugs with plasma proteins. *Drug Metabolism and Pharmacokinetics*, 20(5):309-323.
<https://doi.org/10.2133/dmpk.20.309>.
- [16]. Zhang, G, Chen, X, Guo, J, Wang, J. 2009. Spectroscopic investigation of the interaction between chrysin and bovine serum albumin. *Journal of Molecular Structure*; 921(1-3):346-351.
<https://doi.org/10.1016/j.molstruc.2009.01.036>.
- [17]. Trott, O, Olson, AJ. 2010. AutoDock Vina: improving the speed and accuracy of docking with a new scoring function, efficient optimization, and multithreading. *Journal of Computational Chemistry*; 31(2):455-461.
<https://doi.org/10.1002/jcc.21334>.
- [18]. Masand, VH, Rastija, V. 2017. PyDescriptor: A new PyMOL plugin for calculating thousands of easily understandable molecular descriptors. *Chemometrics and Intelligent Laboratory Systems* 169:12-18. <https://doi.org/10.1016/j.chemolab.2017.08.003>.
- [19]. Studio D. 2008. "Discovery studio" Accelrys [21]. 2008. <https://discover.3ds.com/discovery-studio-visualizer-download>.
- [20]. Lipinski, CA. 2004. Lead-and drug-like compounds: the rule-of-five revolution. *Drug Discovery Today: Technologies*; 1(4):337-341.
<https://doi.org/10.1016/j.ddtec.2004.11.007>.
- [21]. Job, P. 1928. Job's plot analyses for the 2-CG and 3-CG complexes were consistent with 1: 1 stoichiometry. *Annalen der Chemie*; 9:113-34.
- [22]. Latif, A. D., Gonda, T., Vágvölgyi, M., Kúsz, N., Kulmány, Á., Ocsosvski, I., Hunyadi, A. 2019. Synthesis and in vitro antitumor activity of naringenin oxime and oxime ether derivatives. *International Journal of Molecular Sciences*; 20(9), 2184.
<https://doi.org/10.3390/ijms20092184>
- [23]. Ferreira, R. J., Gajdacs, M., Kincses, A., Spengler, G., Dos Santos, D. J., Ferreira, M. J. U. 2020. Nitrogen-containing naringenin derivatives for reversing multidrug resistance in cancer. *Bioorganic & Medicinal Chemistry*, 28(23), 115798.
<https://doi.org/10.1016/j.bmc.2020.115798>
- [24]. Yılmaz, AŞ, Uluçam, G. 2023. Novel N-benzyl-2-oxo-1, 2-dihydrofuro [3, 4-d] pyrimidine-3 (4H)-carboxamide as anticancer agent: Synthesis, drug-likeness, ADMET profile, DFT and molecular modelling against EGFR target. *Heliyon*; e12948.
<https://doi.org/10.1016/j.heliyon.2023.e12948>.
- [25]. Hu, Y. J., Wang, Y., Ou-Yang, Y., Zhou, J., & Liu, Y. 2010. Characterize the interaction between naringenin and bovine serum albumin using spectroscopic approach. *Journal of Luminescence*, 130(8), 1394-1399.
<https://doi.org/10.1016/j.jlumin.2010.02.053>
- [26]. Liu, J., Yang, Z., Cheng, Y., Wu, Q., He, Y., Li, Q., & Cao, X. 2020. Eriodictyol and naringenin inhibit the formation of AGEs: An in vitro and molecular interaction study. *Journal of Molecular Recognition*, 33(1), e2814.
<https://doi.org/10.1002/jmr.2814>
- [27]. Daina, A, Michielin, O, Zoete, V. 2017. SwissADME: a free web tool to evaluate pharmacokinetics, drug-likeness and medicinal chemistry friendliness of small molecules. *Scientific Reports*; 7(1):42717.
<https://www.nature.com/articles/srep42717>.